Low-lying GT$^+$ strength in ^{64}Co studied via the ^{64}Ni(d,^{2}He)^{64}Co reaction

L. Popescu,[1,2,*] C. Bäumer,[3] A. M. van den Berg,[1] D. Frekers,[3] D. De Frenne,[2] Y. Fujita,[4] E. W. Grewe,[3] P. Haefner,[3] M. N. Harakeh,[1] M. Hunyadi,[1] M. A. de Huu,[1] E. Jacobs,[2] H. Johansson,[5] A. Korff,[3] A. Negret,[2,*] P. von Neumann-Cosel,[6] S. Rakers,[3] A. Richter,[6] N. Ryezayeva,[6] A. Shevchenko,[6] H. Simon,[5] and H. J. Wörtche[1]

[1]*Kernfysisch Versneller Instituut, University of Groningen, Zernikelaan 25, NL-9747 AA Groningen, The Netherlands*

[2]*Vakgroep Subatomaire en Stralingsfysica, Universiteit Gent, B-9000 Gent, Belgium*

[3]*Institut für Kernphysik, Westfälische Wilhelms-Universität Münster, D-48149 Münster, Germany*

[4]*Department of Physics, Osaka University, Toyonaka, Osaka 560-0043, Japan*

[5]*Gesellschaft für Schwerionenforschung mbH, D-64291 Darmstadt, Germany*

[6]*Institut für Kernphysik, Technische Universität Darmstadt, Germany*

(Received 4 May 2006; revised manuscript received 1 September 2006; published 9 May 2007)

The ^{64}Ni(d,^{2}He)^{64}Co reaction was studied at the AGOR cyclotron of KVI, Groningen, with the Big-Bite Spectrometer and the EuroSuperNova detector using a 171-MeV deuteron beam. An energy resolution of about 110 keV was achieved. In addition to the $J^\pi = 1^+$ ground state, several other 1^+ states could be identified in ^{64}Co and the strengths of the corresponding Gamow-Teller transitions were determined. The obtained strength distribution was compared with theoretical predictions and former (n, p) experimental results and displayed a good agreement. Due to the good energy resolution, detailed spectroscopic information was obtained, which supplements the data base needed for network calculations for supernova scenarios.

DOI: 10.1103/PhysRevC.75.054312 PACS number(s): 25.55.Kr, 23.40.−s, 26.50.+x, 27.50.+e

I. INTRODUCTION

The spin-isospin response of nuclei can be successfully investigated via (p, n)- and (n, p)-type charge-exchange (CE) reactions [1]. At intermediate incident energies and zero-momentum transfer the reaction cross section is dominated by the spin-isospin component of the central part of the nucleon-nucleon effective interaction [2,3]. This is approximatively satisfied for scattering angles close to 0°. Furthermore, transitions with $\Delta L = 0$ peak at 0°. As a consequence, under these experimental conditions, the measured transitions are mainly characterized by: $\Delta S = 1$, $\Delta T = 1$, $\Delta L = 0$. By analogy to the allowed β-decay, these transitions are called Gamow-Teller (GT) transitions. They are connected to the weak nuclear transitions and allow the investigation of excitation energy regions inaccessible to β decay. Under the mentioned conditions, the CE reaction cross section is expected to become proportional to the GT transition strength, B(GT) [1,4].

Due to their importance as input data in the modeling of supernovae explosions, the strengths of GT transitions in the β^+ direction, B(GT$^+$), in fp-shell nuclei like ^{64}Co, are highly demanded (see, e.g., Refs. [5,6] and references therein). It was shown, e.g., for ^{58}Co [5], that the electron-capture rates depend strongly on the fine structure of the GT strength at low excitation energies.

For an experimental study of the GT strength distribution in ^{64}Co, we have chosen the ^{64}Ni(d,^{2}He)^{64}Co reaction. This is an (n, p)-type reaction, which, compared to the pure (n, p) reaction, presents the advantage of a much better energy resolution, achievable due to the acceleration of charged particles delivered in a primary beam. The (d,^{2}He) reaction cross section is dominated by spin-flip transitions: the deuteron is mainly in a triplet state, whereas the detected proton-pairs, originating from ^{2}He particles with an internal energy limited to $\epsilon \leqslant 1$ MeV in our experiments, are mainly in a singlet state. The higher partial waves contributions are estimated to be only of the order of a few percentages [7].

The proportionality between the (d,^{2}He) reaction cross section and the B(GT$^+$) was shown, e.g., in Refs. [8,9], that describe a systematic study on a series of nuclei with $6 \leq A \leq 32$. For higher masses this proportionality is not yet proven and case-by-case calibration is necessary, as is done for the case of ^{64}Co.

II. EXPERIMENT

The ^{64}Ni(d,^{2}He)^{64}Co experiment was performed at the KVI, Groningen, with a 171-MeV deuteron beam extracted from the superconducting AGOR cyclotron. The outgoing proton pairs from the ^{2}He particles were momentum analyzed by the Big-Bite Spectrometer (BBS) [10] and measured with the EuroSuperNova (ESN) detector. A detailed description of the (d,^{2}He) experiment, the detector, electronics, and data-acquisition system as well as the data analysis is given in Refs. [11–16].

Measurements with three spectrometer angle settings, $\theta_{\text{lab}} = 0°$, 3°, and 5°, were performed. The solid angle acceptance in mode B [10], which was used in the present setup, is 9.2 msr. However, the ESN detector limited the acceptances to $\Delta\theta = 1.4°$ and $\Delta\phi = 4.3°$. Due to this large acceptance it was possible to generate spectra with different scattering-angle gates. A precise determination of the scattering angles requires good angular resolution both horizontally and vertically. Typical angular resolutions achievable with the ESN detector in conjunction with BBS in (d,^{2}He) experiments

[*]Permanent address: NIPNE, Bucharest, Romania.

are better than 0.5° (FWHM) for the reconstructed ^{2}He particles. Because of the large vertical opening angle, this allowed at 0° to generate two spectra: one for $\theta_{\text{c.m.}} \leqslant 1°$ and the other for $1° \leqslant \theta_{\text{c.m.}} \leqslant 2°$. At the other BBS angles, we generated spectra imposing the condition $2.5° \leqslant \theta_{\text{c.m.}} \leqslant 4.5°$ and $4.5° \leqslant \theta_{\text{c.m.}} \leqslant 6.5°$. The size of the angular bin was constrained by the rather poor statistics.

A self-supporting ^{64}Ni foil with an isotopic purity of 96.48% and thickness of 5.2 mg/cm^2 was used as target. The main contaminants in the target were ^{58}Ni (1.89%), ^{60}Ni (1.10%), and ^{62}Ni (0.45%). Given the very small admixtures of the contaminants, they are not expected to contribute significantly to the ^{64}Co spectrum. Moreover, the more negative Q value of the ^{64}Ni(d,^{2}He) reaction essentially separates the ^{64}Co levels from the low-energy levels reported in the literature for the three contaminants.

The beam currents ranged between 0.3 and 2 nA, depending on the BBS angle. At $\theta_{\text{lab}} = 0°$ these current limitations were mainly imposed by background contributions to the spectra (see Sec. III). The prompt to random ratio for this measurement, when imposing the corresponding gates on the acquired data, was about 3 to 1. Furthermore, at any setting of the BBS the count rate to deadtime ratio imposes a limit on the current. For the 3° and 5° BBS angle settings the local beam-stop in the scattering chamber is used, which imposes a second limit, due to radiation damage to the electronics, which, in this case, limits the current even if the count rate to deadtime ratio is acceptable.

By using the *momentum dispersion-matching* technique [17], an energy resolution $\Delta E \approx 110$ keV (FWHM) was achieved for the 0° spectrum. This is about a factor of 8 better than what was achieved in a former ^{64}Ni(n, p) experiment [18], allowing now the separation of several individual states in the low excitation energy region.

III. DATA ANALYSIS AND EXPERIMENTAL RESULTS

A first step in the data analysis is the experimental background subtraction. Especially at very forward scattering angles, the detection of the two protons from ^{2}He takes place in the presence of a huge proton background originating mainly from the deuteron break-up, with a cross section of several orders of magnitude higher than the one of (d,^{2}He) reaction [13]. For the experimental background reduction the time difference between the two detected protons in an event is used. Prompt coincidences are selected and the amount of the contributions from random coincidences is determined and subtracted; see Fig. 1. For a detailed description of this procedure, see Refs. [13,15,16]. The random coincidences subtraction induces a small uncertainty of less than 5%, which is included when estimating the systematic uncertainty on the absolute cross sections.

As there is not much information available in the literature regarding the level scheme and J^{π} values of ^{64}Co, the identification of GT transitions in our study was based on an angular distribution analysis in which the experimental cross sections were compared with DWBA calculations. Because of the selectivity of the (d,^{2}He) reaction [13], transitions with a

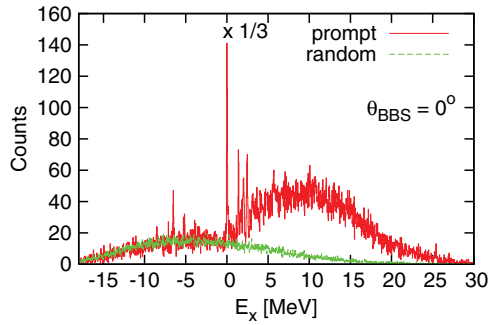

FIG. 1. (Color online) The ^{64}Co spectrum taken at 0° when the gate on prompt coincidences is imposed. For a better view of the spectrum, the ground-state peak was scaled down by a factor of 3. The random-coincidence spectrum is overlapped. Corrections for the limited spectrometer and detector acceptances for the two-proton system (see text for details) are not included. The peak around $E_x = -6.5$ MeV is generated by a small contamination of the target with hydrogen. From about $E_x = -5.1$ MeV there are very small contributions from the ^{58}Ni component in the target.

$\Delta L = 0$ character in the low-exitation-energy region are GT transitions. Spectra with different scattering-angle gates have been produced (see Fig. 2) from the measurements taken with the three BBS angular settings.

Relative (ideally, absolute) differential cross sections are needed for analyzing the angular distributions and calculating the corresponding GT^{+} strengths. Therefore, the cross-section

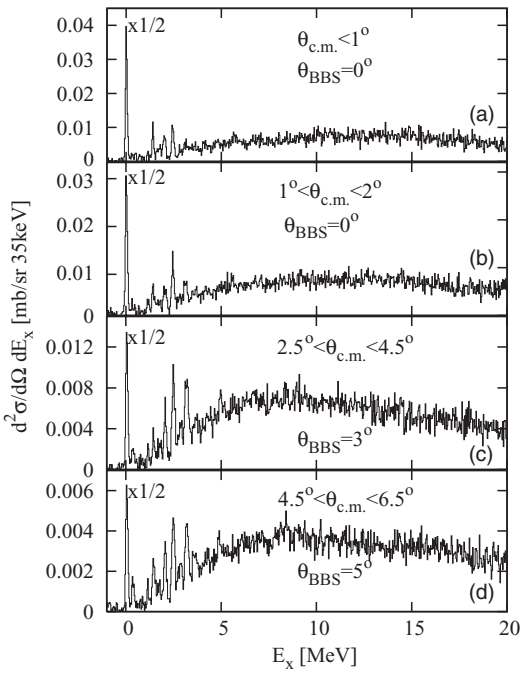

FIG. 2. Double-differential cross sections of the ^{64}Ni(d,^{2}He)^{64}Co reaction for different scattering-angle gates. The BBS angular settings as well as the scattering-angle gates are indicated in the figure. Because of the considerable difference in intensities between the ground-state peak and the rest of the spectra, the ground-state peak was scaled by a factor of 1/2.

spectra had to be corrected for the limited acceptance of the spectrometer and detection system for the proton pair. The correction function was determined via a Monte Carlo simulation taking into account the coincident detection of the two protons within the solid angle and momentum acceptance. The specific correction function for every experimental setting and angular bin was determined. Refs. [13,15,16] give a detailed description of this procedure.

The overall estimation of the uncertainty on the absolute value of the cross sections was determined to be of the order of 15%. The main uncertainty, about 10%, is introduced by the estimation of the spectrometer and detector acceptance for the two-proton system. As mentioned earlier, uncertainties introduced by the subtraction of the random coincidences are also contributing, as well as uncertainties in measuring the beam current, detector efficiency, target thickness, and target enrichment.

As seen in Fig. 2, starting from around 2.5 MeV, the spectra are dominated by a bumplike structure. This bump contains several contributions. Starting from around the threshold energy for the decay by neutron emission (S_n = 6.02 MeV), background contributions generated by the quasi-free scattering (QFS) have to be taken into account. Because of the Fermi motion of nucleons inside the nucleus, this region is very broad [19,20]. The very broad giant resonances like the isovector spin giant dipole resonance (IVSGDR, expected around 9 MeV [21]) and the isovector spin giant monopole resonance (IVSGMR, expected around 20 MeV [21]) are overlapping with this continuum. The long tails of these resonances contribute to the low-energy region of the spectra. As expected, e.g., from a typical $\Delta L = 1$ angular distribution (characterizing the IVSGDR), these contributions increase with increasing scattering angle. Such behavior is easily observed by examining the low-excitation-energy region of the spectra in Fig. 2.

We assumed that all the contributions discussed above can be estimated by a curve connecting the valleys in the spectra (see the upper panel in Fig. 4) and subtracted. The energy region $E_x \leqslant 5$ MeV of the resulting spectra has been decomposed into individual peaks by using the fitting program `fityk` [22]. No significant difference was observed when choosing the Gaussian shape or using the so-called Voigt function (composed by a Gaussian plus exponential tails) for the peak shape. Because the energy resolution achieved in this experiment allowed the separation of the ground-state peak from the other peaks corresponding to known levels and because it is not expected for the levels in the excitation energy region below the particle decay threshold to have an observable natural width, the width determined for the ground-state peak was imposed when analyzing the other peaks. The results of the fits for two spectra at different angles ($\theta_{\text{c.m.}} \leqslant 1^\circ$ and $4.5^\circ \leqslant \theta_{\text{c.m.}} \leqslant 6.5^\circ$) when using the Gaussian shape are presented in Figs. 3 and 4.

The locations of the centroids for several peaks are indicated in the figures. Apart from the 1.974-MeV level, all the observed levels below 2.1 MeV were reported in the literature [23]. In the compiled data, there is no information concerning higher energy states. The levels observed in our study are listed in Table I.

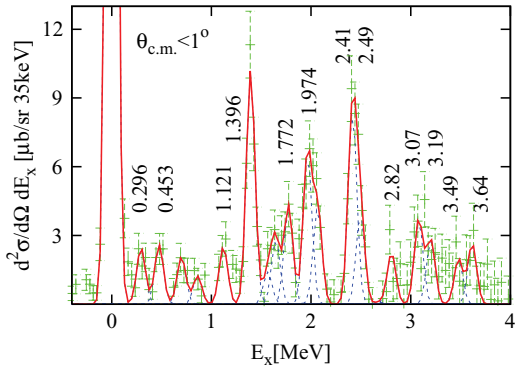

FIG. 3. (Color online) Fit of the $E_x \leqslant 4$ MeV energy region of the $\theta_{\text{c.m.}} \leqslant 1^\circ$ spectrum. The contribution of QFS and giant resonances to the spectrum has been estimated by a curve connecting the minima in the spectrum (as shown in the upper panel of Fig. 4) and subtracted (see text for details). The error bars are statistical only. Centroids of peaks corresponding to several states below 4 MeV are indicated.

Figures 5 and 6 show the experimental cross sections for seven discrete transitions and the energy-integrated cross sections for five excitation energy intervals containing the triplet around 1.6 MeV and the doublets around 2, 2.4, 2.7, 3.1, and 3.6 MeV together with the results of DWBA model calculations, using the code ACCBA of Okamura [24]. In calculating the cross sections for different ΔL components it was assumed that the $\Delta L = 0$ component involves $J^\pi = 1^+$, the $\Delta L = 1$ $J^\pi = 1^-$, and the $\Delta L = 2$ $J^\pi = 3^+$ final states. Assuming a small variation with the mass number, the entrance channel of the reaction was described in the DWBA code through optical-model parameters determined in a deuteron elastic-scattering experiment on ^{58}Ni [25]. For the exit channel optical-potential parameters were calculated from a global fit to proton elastic-scattering data for incident energies of 80–180 MeV [26]. As effective two-body interaction

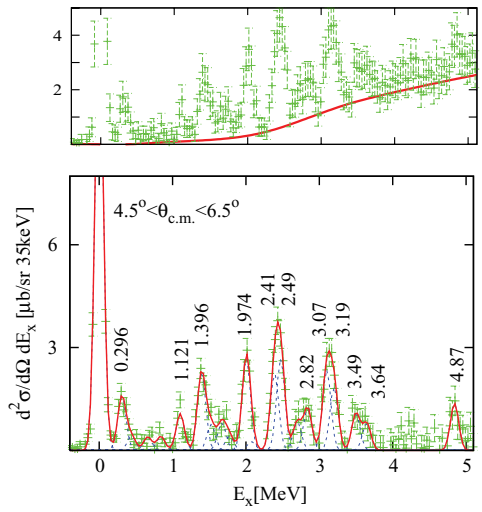

FIG. 4. (Color online) Fit of the $4.5^\circ < \theta_{\text{c.m.}} < 6.5^\circ$ spectrum. The upper panel shows our estimation of the contributions from giant resonances and QFS (see text for details) that have been subtracted from the initial spectrum. The error bars are statistical only. Centroids of peaks corresponding to several states are indicated.

TABLE I. $B(\mathrm{GT}^+)$ of transitions to $J^\pi = 1^+$ states in ^{64}Co observed in the ^{64}Ni$(d,^2\mathrm{He})^{64}$Co reaction. The ratio $\mathcal{R} = \sigma^{\Delta L=0}(0.5^\circ)/\sigma^{\mathrm{tot}}$ denotes the $\Delta L = 0$ fraction of the total cross section at $\theta_{\mathrm{scatt}} = 0.5^\circ$. The $B(\mathrm{GT}^+)$ value for the ground-state transition corresponds to the calibration value determined in Eq. (2). The uncertainty in the cross section of this level is further propagated in the uncertainty of the obtained unit cross section.

$E_x^{\mathrm{literature}}$ (MeV)	E_x (MeV)	$\sigma^{\Delta L=0}_{(d,^2He)}(0.5^\circ)$ (mb/sr)	$\mathcal{R}$	$B(\mathrm{GT}^+)$
0.000	0.000	0.301(49)	1.00	0.627 ± 0.036[a]
0.311(15)	0.296(22)	0.006(4)	0.54	0.013 ± 0.010
0.463(15)	0.453(21)	0.010(2)	1.00	0.021 ± 0.006
0.703(15)	0.678(21)	0.008(1)	1.00	0.018 ± 0.005
0.867(15)	0.836(24)	0.004(2)	0.80	0.009 ± 0.005
1.144(15)	1.121(18)	0.009(6)	0.83	0.021 ± 0.013
1.423(15)	1.396(15)	0.041(4)	1.00	0.093 ± 0.021
1.541(15)	1.543(20)	0.029(6)	0.97	0.066 ± 0.019
1.687(15)	1.650(22)			
1.806(30)	1.773(15)			
2.051(15)	1.974(26)	0.036(8)	0.95	0.085 ± 0.026
	2.065(29)			
	2.413(23)	0.045(11)	0.89	0.108 ± 0.035
	2.494(20)			
	2.681(20)	0.007(1)	0.74	0.017 ± 0.005
	2.817(23)			
	3.074(30)	0.022(9)	0.81	0.055 ± 0.026
	3.188(30)			
	3.486(20)	0.019(7)	0.90	0.049 ± 0.021
	3.644(27)			

[a]Determined from the log*ft* value; Ref. [23].

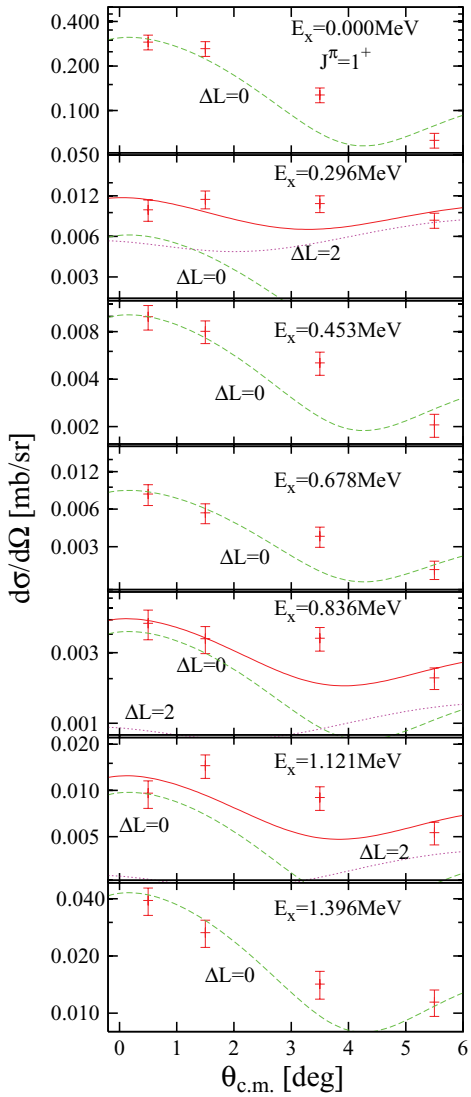

FIG. 5. (Color online) Fit of the experimental angular distributions of the differential cross section for the peaks below 1.5 MeV. The shapes for different ΔL are obtained in a DWBA calculation (see text). The indicated errors on the experimental points account for statistical errors, uncertainties induced by the correction for the limited acceptance of the detection system for the proton pair and uncertainties in the fitting procedure.

parameters, the central and the tensor part from the T matrix parametrization at 100 MeV from Franey and Love [3] were applied. One-body transition densities were calculated in the normal-mode formalism with the program NORMOD [27].

The calculated cross sections were scaled to match the experimental cross sections. In these calculations, the $\sigma\tau$ and $T\tau$ amplitudes due to microscopic wave functions have, of course, been added coherently. However, the effect of the latter term could not be accurately determined in the present analysis. Where the fit to the experimental data was not good, an incoherent $\Delta L = 2$ contribution has been added [28], which has been further used in estimating the uncertainties in GT strength due to the effects of the coherent $\Delta L = 2$ contribution.

As the four experimental values are obtained from different measurements, by defining different acceptance functions of the detection system for the proton pair, the estimation of 10% uncertainty of the acceptance correction function has to be included when analyzing angular distributions. Apart from this, the error bars given in Figs. 5 and 6 and included in the angular-distribution analysis account for statistical errors and uncertainties induced by the fitting procedure. A systematic deviation of the experimental points at 3.5° is observed. This deviation can be caused by a larger imprecision in measuring the integrated current for the $\theta_{\mathrm{BBS}} = 3^\circ$ setting. A detailed investigation of our data and recorded information did not uncover the source of this deviation.

The angular distribution of the peak corresponding to the ground-state transition (a known $J^\pi = 1^+$ state) is fitted well by the calculated $\Delta L = 0$ shape. This is the strongest GT transition to an individual level in ^{64}Co.

There are several other peaks having an angular distribution with a $\Delta L = 0$ character: at 0.453, at 0.678, and at 1.396 MeV. A $J^\pi = 1^+$ spin and parity for the corresponding levels can be deduced. The small peaks at 0.836 and 1.121 MeV are fitted reasonably well by a mixture of $\Delta L = 0$ and $\Delta L = 2$ components allowing $J^\pi = (1, 2, \text{or } 3)^+$ for the corresponding levels.

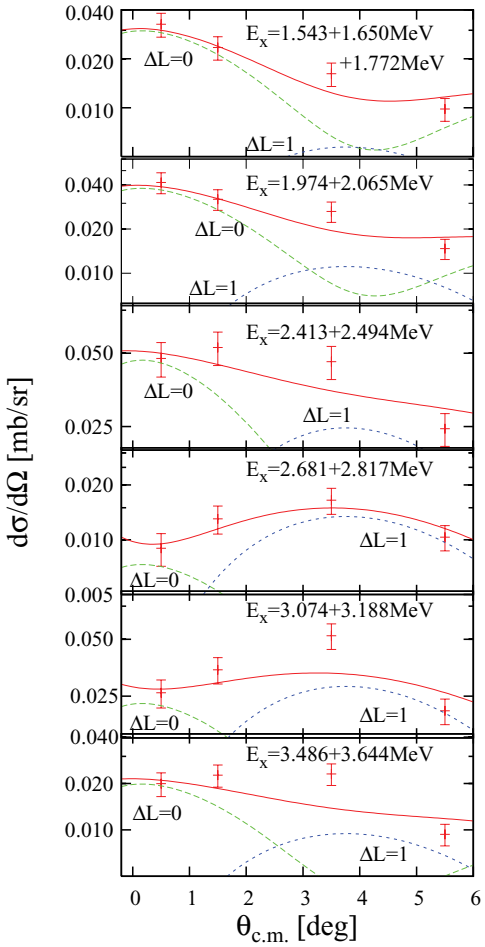

FIG. 6. (Color online) Fit of the experimental angular distributions of the differential cross section for the selected groups of levels. The shapes for different ΔL are obtained in a DWBA calculation (see text). The indicated errors on the experimental points account for statistical errors, uncertainties induced by the correction for the limited acceptance of the detection system for the proton pair and uncertainties in the fitting procedure.

It was suggested by Runte *et al.* [29] in a study of the β decay of ^{64}Fe to ^{64}Co, that, apart from the ground state, a second 1^+ level is present at about 311 keV in ^{64}Co. The energy resolution achieved in our (d,^{2} He) experiment allowed the separation of this peak, present in the ^{64}Co spectrum at $E_x = 296 \pm 22$ keV. But the angular distribution analysis suggests a $\Delta L = 2$ component stronger than the $\Delta L = 0$ one for the corresponding transition. Even if this peak would have a $\Delta L = 0$ component, as assumed in the fit from Fig. 5, the fraction of the GT strength exhausted by this weak transition would be extremely small. The GT component contributing to this peak could, in fact, be due to contributions from the ground-state or the 453-keV level, whose angular distributions have a clear $\Delta L = 0$ character. The $\Delta L = 2$ character of the transition to the 296-keV level is of particular importance as Williams *et al.* [18], in a previous (n, p) study on ^{64}Ni, deduced a possible 40% contribution of the transition to this level to the ground-state peak when determining the unit cross section [see Eq. (1)]. The energy resolution of the (n, p) measurement was around 800 keV. Therefore, in their case the ground-state peak contained also contributions from the other levels at low excitation energy. The experimental unit cross section in the (n, p) study was 5.37 ± 0.39 mb/sr when no contributions from other low-excitation-energy states to the ground-state peak were considered and 3.2 ± 0.9 mb/sr when considering a 40% $\pm$ 16% contribution. However, our results indicate no significant $\Delta L = 0$ cross section in the excitation energy region 100–800 keV.

In the energy region 1.5–4 MeV several overlapping peaks are observed and the deduced cross section, especially for the small peaks, is strongly dependent on the fitting procedure. Consequently, the uncertainties on the determined individual cross sections are large and it was preferred to determine the GT component included in the multiplets, rather than doing it for the individual peaks. The fits of the angular distributions for these groups of levels are shown in Fig. 6. The experimental distributions are fitted with rather good accuracy by assuming a mixture of $\Delta L = 0$ and $\Delta L = 1$ components.

For the calculation of the strengths of the identified GT transitions the proportionality between the reaction cross section and the B(GT) was used [4]:

$$\sigma(q, \omega) = \hat{\sigma}(E_{\text{beam}}, A) F(q, \omega) B(\text{GT}). \quad (1)$$

The proportionality factor $\hat{\sigma}$ is called "unit cross section" and it is a function of the beam energy and the nature of the target. In our case, it was determined directly from the cross section of the ground-state transition, for which the B(GT$^+$) is obtained from the $\log ft = 4.3$ value for the inverse transition measured in β decay [23] and taking into account the reversed initial and final states:

$$B(\text{GT}^+) = \frac{2J_f + 1}{2J_i + 1} \frac{6166 \pm 2s}{\left(\frac{g_A}{g_V}\right)^2 ft} = 0.627 \pm 0.036. \quad (2)$$

Here, $(g_A/g_V) = -1.266 \pm 0.004$ [30] and J_i and J_f are the spins of the initial and final states in the ^{64}Ni(d,^{2} He)^{64}Co reaction.

The factor $F(q, \omega)$ in Eq. (1) accounts for the extrapolation of the cross section to zero momentum transfer $q = 0$ and zero energy loss $\omega = 0$. It goes to 1 at vanishing momentum transfer and energy loss [4]. It was deduced via DWBA calculations:

$$F(q, \omega) = \frac{\sigma_{\text{DWBA}}(q, \omega)}{\sigma_{\text{DWBA}}(q = 0, \omega = 0)}. \quad (3)$$

This factor is about 0.7 for the ground-state transition and decreases to about 0.6 at $E_x = 3.6$ MeV.

The calculated B(GT$^+$) values are included in Table I. Based on our previous experience with (d,^{2}He) and (^{3}He, t) studies, we expect good proportionality for transitions characterized by $B(\text{GT}) \geqslant 0.04$ units (see, e.g., Ref. [32]). Therefore, the error bars for the determined values below this limit might be underestimated.

IV. DISCUSSION

Figure 7 compares the present results with the theoretical large-scale shell model (LSSM) calculations of Caurier *et al.* employing a slightly monopole-corrected version of the

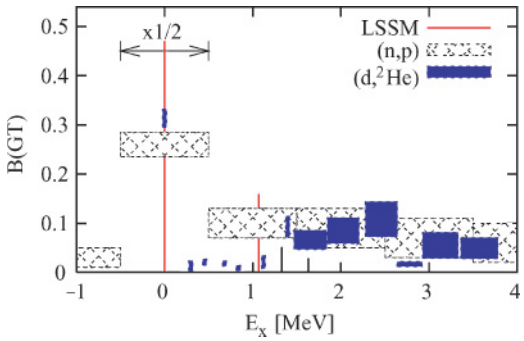

FIG. 7. (Color online) The experimental $B(\mathrm{GT}^+)$ distribution for $E_x \leqslant 4$ MeV together with the (n, p) results as shown in Fig. 12 of Ref. [18] and the LSSM calculations of the GT^+ strength from ^{64}Ni to individual levels [31]. A quenching factor $q = 0.74$ was utilized for scaling the shell-model amplitudes. The block widths represent the integrated energy region and the block heights are proportional to the uncertainty on the $B(\mathrm{GT})$ value. The error bars on the (n, p) data are statistical only. For a better observation, the strength corresponding to the ground-state transition was scaled by 1/2 for both theoretical and experimental results.

KB3 interaction [31]. The model space was reduced to the *fp* shell (including $1f7/2$, $2p3/2$, $2p1/2$, and $1f5/2$ orbitals), the truncation level involving about 10 million configurations. A quenching factor $q = 0.74$ was utilized for scaling the shell-model amplitudes [31]. The (n, p) results of Williams *et al.* as given in Fig. 12 of Ref. [18] are also shown for comparison. Because the strength for the ground-state transition as deduced from the β-decay measurement [see Eq. (2)] is not accurately described by the (n, p) data (see Fig. 7), we assume that these $B(\mathrm{GT}^+)$ values are obtained in the (n, p) study by employing the unit cross section of about 4 mb/sr calculated with Eq. (2) given in Ref. [18], which represents a parametrization as function of the beam energy and target mass. In all three distributions most of the strength is concentrated in the ground-state transition, but the shell-model calculations overestimate its value by about 50%. The difference in strength is almost entirely fragmented over several states in the $(d, ^2\mathrm{He})$ data.

For a better comparison, the running sums are plotted in Fig. 8. It becomes obvious that a better agreement could be obtained between $(d, ^2\mathrm{He})$ and (n, p) experimental distributions if the latter one is scaled by a factor of $\sim$1.2. This factor has been obtained as the ratio between the total $B(\mathrm{GT})$ strength of 1.72 ± 0.09, as quoted in the text by Williams *et al.* [18] and shown in the running sum plot in Fig. 10 of the same article, in comparison with the integrated $B(\mathrm{GT})$ strength of about 1.4, which can be deduced from Fig. 12 of the same article. This might suggest an inconsistent application of unit cross sections in the (n,p) analysis. In the present article, the data presented in Fig. 12 of Ref. [18] are used for comparison.

Nevertheless, it should be noticed that the $B(\mathrm{GT}^+)$ values obtained in our study are based on the assumption that there are no GT contributions to the estimated "background" (see Fig. 4) that has been subtracted. This is only a simple assumption, without any theoretical support. Therefore, our results should be regarded as lower limit rather than absolute

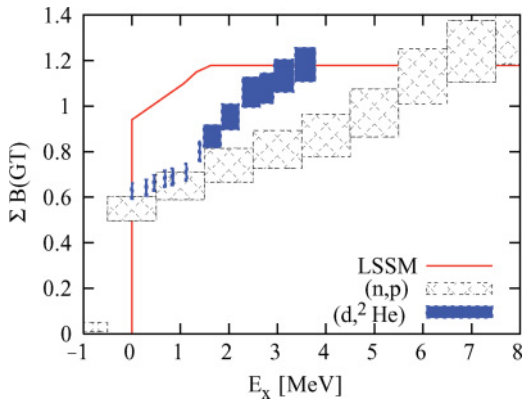

FIG. 8. (Color online) Cumulative sum of $B(\mathrm{GT}^+)$ values from the $(d, ^2\mathrm{He})$ experiment, the (n, p) experiment as deduced from Fig. 12 of Ref. [18] and the LSSM calculations [31]. The block widths represent the integrated energy region and the block heights are proportional to the uncertainty on the $\sum B(\mathrm{GT}^+)$. The error-bars on the (n, p) data are statistical only.

values. As mentioned by the authors of Ref. [31], a better description can be obtained in the calculations if the $1g9/2$ orbital is included in the model space.

The spectroscopic information supplied by the present study is contained in Fig. 9, which presents a comparison with the information available in the literature at this moment. The left column shows the different levels found in the present $(d, ^2\mathrm{He})$ experiment. The central column indicates levels obtained in the $(t, ^3\mathrm{He})$ study by Flynn and Garrett [33] and the right column levels deduced in the γ-decay study of a $T_{1/2} = 6.4 \pm 3.0$ ns isomer in ^{64}Co by Asai *et al.* [34]. The suggested J^π values are indicated at the left side of the levels.

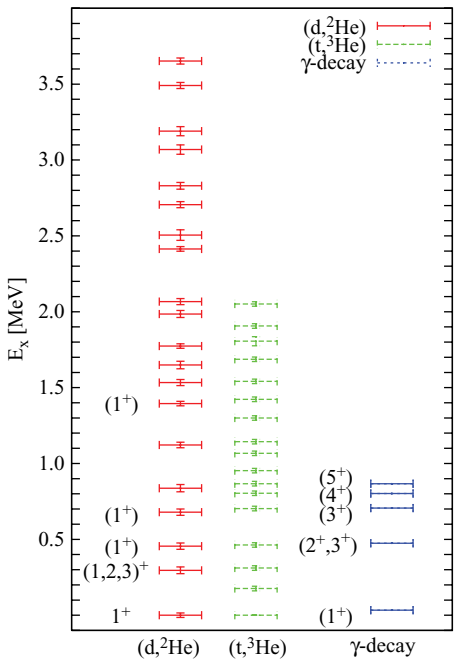

FIG. 9. (Color online) Comparison of the ^{64}Co level scheme obtained in this study with the ^{64}Ni$(t, ^3\mathrm{He})$ results and γ-decay results shifted by 33 keV (see text). Suggested J^π values are indicated.

A good agreement is observed between the $(d,^2\text{He})$ and the $(t,^3\text{He})$ results. Due to the superior energy resolution in the $(t,^3\text{He})$ experiment, there are several levels clearly separated in the $(t,^3\text{He})$ spectra that cannot be observed in the $(d,^2\text{He})$ spectra. This might suggest a higher-order character for the corresponding multipolarities, because the $(t,^3\text{He})$ data were taken at much higher scattering angles, where the $\Delta L = 0$ component is no longer favored.

The level spacings between the 867-, 804-, 703-, 463-, and 0-keV states determined through the $(t,^3\text{He})$ reaction are very similar to the 64–97–232–441 keV cascade γ-ray energies measured in the study of Asai *et al*. By normalizing the isomeric state, placed at 834 keV in the γ study, to the 867-keV level observed in the $(t,^3\text{He})$ experiment, all the levels except the ground state agree in energy within the experimental uncertainties. The energy difference between the lowest-lying state observed in the γ-decay measurement and the ground state measured in the $(t,^3\text{He})$ and $(d,^2\text{He})$ reactions is +33 keV, which could be explained by the existence of an additional state at 33 keV above the ground state. This hypothesis is acceptable as the experimental setup used in the γ-decay measurement could not detect 33-keV γ rays [34]. Furthermore, the energy resolutions achieved in the $(t,^3\text{He})$ and $(d,^2\text{He})$ reactions (50 and 110 keV, respectively) are not sufficient to separate a weakly excited level at 33 keV above the ground state.

The 1^+ character of the 453 ± 21-keV and 678 ± 21-keV states observed in the present experiment contradicts the $(2^+, 3^+)$ and, respectively, (3^+) assignment to the corresponding states in the γ measurement of Asai *et al*. [34]. However, spins and parities in the γ-decay study are based on the assumption that the lowest-lying state observed in the γ-decay measurement is the ^{64}Co ground state, known from β-decay studies to be a 1^+ state [23]. This assumption is not in agreement with the above explanation.

In spite of the limited energy resolution, we tried to decompose the multiplets present in the energy region 1.5 MeV $\leqslant E_x \leqslant$ 5 MeV into individual peaks. The obtained energies for the corresponding levels are indicated in Table I and Fig. 9. An additional level, around 4.87 ± 0.04 MeV is suggested by the fit of the spectra for $2.5^\circ \leqslant \theta_{\text{c.m.}} \leqslant 4.5^\circ$ and $4.5^\circ \leqslant \theta_{\text{c.m.}} \leqslant 6.5^\circ$ (see Fig. 4).

V. CONCLUSION

The GT strengths for transitions to low-lying states in ^{64}Co have been measured via the $^{64}\text{Ni}(d,^2\text{He})^{64}\text{Co}$ reaction. The good resolution of the measurement allows the observation of fine structure in the GT resonance, seen as a broad bump in an earlier (n, p) study [18]. This permits, for the first time, a detailed comparison with the shell-model predictions in the low-excitation-energy region of ^{64}Co. The experimental results suggest a larger fragmentation of the strength than predicted by LSSM calculations. A similar study performed on ^{58}Ni showed that such fragmentation of the strength over low-energy states can have, especially at small temperatures, a large impact on the rates of electron-capture processes taking place in the presupernova stage of a massive star [5]. Because ^{64}Ni contributes to the electron-capture rate in the presupernova stage, the present results can impose constraints in future calculations for the location of the states at low excitation energy.

Good agreement was observed between the $^{64}\text{Ni}(d,^2\text{He})^{64}\text{Co}$ results and the $^{64}\text{Ni}(n, p)^{64}\text{Co}$ results of Williams et al. [18] when the (n, p) results were normalized by a factor of 1.2.

Also new spectroscopic information was obtained: $J^\pi = 1^+$ was suggested for the levels at 0.453(21) MeV, 0.678(21) MeV, and 1.396(15) MeV. Indications for the existence of several new levels are given.

ACKNOWLEDGMENTS

The authors are grateful to the accelerator group of KVI for providing a high-quality deuterium beam. This work was performed as part of the research program of the Fund for Scientific Research—Flanders. It was also supported by the EU under EURONS within the 6th framework under contract RII3-CT-2005-506065 and by DFG, Germany, under contract SFB634.

[1] F. Osterfeld, Rev. Mod. Phys. **64**, 491 (1992).
[2] W. G. Love and M. A. Franey, Phys. Rev. C **24**, 1073 (1981).
[3] M. A. Franey and W. G. Love, Phys. Rev. C **31**, 488 (1985).
[4] T. Taddeucci, C. Goulding, T. Carey, R. Byrd, C. Goodman, C. Gaarde, J. Larsen, D. Horen, J. Rapaport, and E. Sugarbaker, Nucl. Phys. **A469**, 125 (1987).
[5] M. Hagemann, A. M. van den Berg, D. D. Frenne, V. M. Hannen, M. N. Harakeh, J. Heyse, M. A. de Huu, E. Jacobs, K. Langanke, G. Martínez-Pinedo, *et al*., Phys. Lett. **B579**, 251 (2004).
[6] K. Langanke and G. Martínez-Pinedo, Rev. Mod. Phys. **75**, 819 (2003).
[7] S. Kox, J. Carbonell, C. Furget, T. Motobayashi, C. Perrin, C. Wilkin, J. Arvieux, J. P. Bocquet, A. Boudard, G. Gaillard *et al*., Nucl. Phys. **A556**, 621 (1993).
[8] S. Rakers, C. Bäumer, A. M. van den Berg, D. Frekers, D. D. Frenne, Y. Fujita, M. Hagemann, V. Hannen, M. N. Harakeh, J. Heyse *et al*., Phys. Rev. C **65**, 044323 (2002).
[9] E. W. Grewe, C. Bäumer, A. M. van den Berg, N. Blasi, B. Davids, D. D. Frenne, D. Frekers, P. Haefner, M. N. Harakeh, M. Hunyadi *et al*., Phys. Rev. C **69**, 064325 (2004).
[10] A. M. van den Berg, Nucl. Instrum. Methods B **99**, 637 (1995).
[11] M. Hagemann, R. Bassini, A. M. van den Berg, F. Ellinghaus, D. Frekers, V. M. Hannen, T. Häupke, J. Heyse, E. Jacobs, M. Kirsch *et al*., Nucl. Instrum. Methods A **437**, 459 (1999).
[12] H. Wörtche, Nucl. Phys. **A687**, 321c (2001).
[13] S. Rakers, F. Ellinghaus, R. Bassini, C. Bäumer, A. M. van den Berg, D. Frekers, D. D. Frenne, M. Hagemann, V. M. Hannen, M. N. Harakeh *et al*., Nucl. Instrum. Methods A **481**, 253 (2002).
[14] V. M. Hannen, R. Bassini, A. M. van den Berg, N. Blasi, D. D. Frenne, R. D. Leo, F. Ellinghaus, D. Frekers, M. Hagemann, M. N. Harakeh *et al*., Nucl. Instrum. Methods A **500**, 68 (2003).

[15] M. Hagemann, C. Bäumer, A. M. van den Berg, D. D. Frenne, D. Frekers, V. M. Hannen, M. N. Harakeh, J. Heyse, M. A. de Huu, E. Jacobs *et al*., Phys. Rev. C **71**, 014606 (2005).
[16] L. Popescu, Ph.D. thesis, Universiteit Gent, 2005.
[17] Y. Fujita, K. Hatanaka, G. P. A. Berg, K. Hosono, N. Matsuoka, S. Morinobu, T. Noro, M. Sato, K. Tamura, and H. Ueno, Nucl. Instrum. Methods B **126**, 274 (1997).
[18] A. L. Williams, W. P. Alford, E. Brash, B. A. Brown, S. Burzynski, H. T. Fortune, O. Häusser, R. Helmer, R. Henderson, P. P. Hui *et al*., Phys. Rev. C **51**, 1144 (1995).
[19] A. Erell, J. Alster, J. Lichtenstadt, M. A. Moinester, J. D. Bowman, M. D. Cooper, F. Irom, H. S. Matis, E. Piasetzky, and U. Sennhauser, Phys. Rev. C **34**, 1822 (1986).
[20] J. Lisantti, F. E. Bertrand, D. J. Horen, B. L. Burks, C. W. Glover, D. K. McDaniels, L. W. Swenson, X. Y. Chen, O. Häusser, and K. Hicks, Phys. Rev. C **37**, 2408 (1988).
[21] S. Nakayama, H. Akimune, Y. Arimoto, I. Daito, H. Fujimura, Y. Fujita, M. Fujiwara, K. Fushimi, H. Kohri, N. Koori *et al*., Phys. Rev. Lett. **83**, 690 (1999).
[22] M. Wojdyr, open Source GPL'd peak profiling program `fityk`, http://www.unipress.waw.pl/fityk.
[23] *Table of Isotopes*, 8th ed., edited by R. Firestone and V. Shirley (Wiley, New York, 1996).
[24] H. Okamura, Phys. Rev. C **60**, 064602 (1999).
[25] C. Bäumer *et al*., Phys. Rev. C **63**, 037601 (2001).
[26] A. Nadasen, P. Schwandt, P. P. Singh, W. W. Jacobs, A. D. Bacher, P. T. Debevec, M. D. Kaitchuck, and J. T. Meek, Phys. Rev. C **23**, 1023 (1981).
[27] S. van der Werf, computer program `NORMOD`, unpublished.
[28] G. Satchler and W. Pinkston, Nucl. Phys. **A411**, 144 (1983).
[29] E. Runte, K.-L. Gippert, W.-D. Schmidt-Ott, P. Tidemand-Peterson, L. Ziegeler, R. Kirchner, O. Klepper, P. O. Larsson, E. Roeckl, D. Schardt *et al*., Nucl. Phys. **A441**, 237 (1985).
[30] K. Schreckenbach, P. Liaud, R. Kossakowski, H. Nastoll, A. Bussiere, and J. P. Guillaud, Phys. Lett. **B349**, 427 (1995).
[31] E. Caurier, K. Langanke, G. Martínez-Pinedo, and F. Nowacki, Nucl. Phys. **A653**, 439 (1999).
[32] Y. Fujita, H. Akimune, I. Daito, H. Fujimura, M. Fujiwara, M. N. Harakeh, T. Inomata, J. Jänecke, K. Katori, A. Tamii *et al*., Phys. Rev. C **59**, 90 (1999).
[33] E. R. Flynn and J. D. Garrett, Phys. Lett. **B42**, 49 (1972).
[34] M. Asai, T. Ishii, A. Makishima, I. Hossain, M. Ogawa, and S. Ichikawa, Phys. Rev. C **62**, 054313 (2000).